

Catalytic oxygen production mediated by smart capsules to modulate elastic turbulence under laminar flow regime

A. Zizzari,^{a†} M. Bianco,^{a†} R. Miglietta,^a L. L. del Mercato,^a M. Carraro,^b A. Sorarù,^b M. Bonchio,^b G. Gigli,^{a,c} R. Rinaldi,^{a,c} I. Viola,^{a,d*}, V. Arima^{a*}

Experimental

Contact angle measurements

Static Contact Angles (SCA) of 0, 0.26, 0.49 and 1.23 M H₂O₂ solutions with and without Ru₄POM-PMCs were measured by the sessile drop method on the substrates used for the device fabrication (PDMS and glass) using a CAM 200 (KSV Instrument Ltd. Finland). The SCA measures were performed onto different areas of three samples for each substrate and the respective averages and standard deviations are shown in Table S2. The SCA values were calculated after 3 min from the preparation to take into consideration the time required for device assembly and solution preparation before performing capillary dynamics studies. The same CAM 200 apparatus was used to allow an approximate estimation of γ_{la} of 0, 0.26, 0.49 and 1.23 M H₂O₂ solutions (without Ru₄POM-PMCs to avoid needle clogging) by pendant drop measurements. The γ_{la} values and the standard deviations reported in Table 2 are an average over 3 drops.

Results and discussion

To verify the correspondence of the experimental data shown in Fig. 2b to the theoretical model and to calculate the temporal range of the actual dynamical regimes inside of the system, a fitting procedure was used.

The analytical expression of the fluid displacement in a micro-channel follows a power-law dynamics which takes into account the confinement effects due to the presence of the walls. The simplified equation is known as a power law of Washburn¹ and can be written as:

$$z(t) = z_0 + (2\Delta p G / \eta)^{1/2} t^{1/2} = z_0 + at^{1/2} \quad (1)$$

where Δp is the Laplace capillary pressure, G is a geometric factor accounting for the channel geometry, η is the effective dynamical viscosity inside the channel^{2,3}. The experimental data are in agreement with the eq. (1) (see Fig. 1b) and the structural and dynamical parameters of the system can be evaluated by a nonlinear regression fitting with the function:

$$y = y_{0i} + a_i x^c \quad (2)$$

where (x, y) are the experimental time data-set and fluid displacement, respectively.

Sample	Starting regime			Intermediate regime		
	y01	a1	c1	y02	a2	c2
H ₂ O	-0.79±0.09	0.38±0.03	0.50±0.01	-1.61±0.24	3.16±0.10	0.15±0.003
	t1 =0-345 s			t2 =345-870 s		
0 M H ₂ O ₂	0.71±0.03	0.49±0.02	0.51±0.01	-3.4±0.2	2.50±0.06	0.25±0.004
	t1 =0-180 s			t2 =180-534 s		
0.26 M H ₂ O ₂	0.31±0.02	0.28±0.02	0.65±0.01	-0.61±0.12	0.99±0.04	0.38±0.01
	t1 =0-97 s			t2 =97-270 s		
0.49 M H ₂ O ₂	0.36±0.02	0.31±0.002	0.66±0.01	-0.17±0.9	0.85±0.03	0.40±0.01
	t1 =0-60 s			t2 =60-660 s		
1.23 M H ₂ O ₂	0.57±0.07	0.46±0.05	0.62±0.02	-0.44±0.05	1.03±0.01	0.41±0.003
	t1 =0-55 s			t2 =55-460 s		

Table S1. Propeller dynamics: fitting analysis

The calculations allowed to reconstruct the fluid dynamic velocity profile (see Fig. 2c) and to distinguish between three different regimes indicated in Fig. 2b:

- *Starting regime* (indicated with *S* in Fig. 2b): In a time interval of about 100 s the systems have reached more or less half of the channel. This regime corresponds to a regime of capillarity ($c = 0.5$) only for pure water and the system without H_2O_2 , while c values > 0.5 were found for the other systems up to a maximum of $c = 0.66$ for the solution 0.49 M of H_2O_2 (see values reported in Table S1).
- *Intermediate regime* (indicated with *I* in Fig. 2b): The dynamics of solutions with Ru_4POM -PMCs undergoes a slow down due to the exhaustion of the pressure difference that supports the motion of the fluid. After the strong acceleration in the initial phase the motion is supported by an elastic pulse which develops along the channel with a high relaxation time.). This behaviour is typical of non-Newtonian fluids.
- Operating plateau (indicated with *P* in Fig. 2b): The flow tends to stop.

To analyse in detail the capillary dynamics of the solutions and evaluate parameters useful to quantitatively describe the observed turbulence phenomena, the interaction of the solution with the microchannel walls and the surface tension γ_{la} at the liquid/air interface have to be calculated. Therefore measurements of SCA and pendant drops were performed. As shown in table S2, the contact angles of aqueous solutions in which Ru_4POM -PMCs are suspended appear smaller than that of pure water or H_2O_2 diluted solutions. The PMCs, which have a positive superficial charge, are probably attracted by both the hydrophilic surfaces which constitute the microfluidic device (glass and PDMS activated with oxygen plasma which expose negatively charged silanol groups) and promote the interactions of the liquid with the surface, thus decreasing the contact angles. The hydrophilicity of solutions with or without capsules slightly decreases with H_2O_2 increase.

	H₂O	0.26M H₂O₂	0.49M H₂O₂	1.23M H₂O₂
Θ_{glass} (°) (no Ru_4POM-PMCs)	44.1±0.9	45.6±0.2	52.2±0.6	54.0±1.5
Θ_{glass} (°) (with Ru_4POM-PMCs)	28.9±0.7	29.3±1.1	30.2±1.0	36.8±1.1
Θ_{PDMS} (°) (no Ru_4POM-PMCs)	0	0	8.7±0.4	11.8±0.8
Θ_{PDMS} (°)(with Ru_4POM-PMCs)	0	0	7.8±1.1	11.8±1.3
γ_{LV} (mN/m) (no Ru_4POM-PMCs)	71.8±0.8	73.4±0.1	74.6±0.7	70.7±0.6

Table S2. Static contact angles on PDMS and glass calculated for 0, 0.26, 0.49 and 1.23 M H_2O_2 solutions without or with Ru_4POM -loaded capsules. γ_{LV} values calculated for pure water and diluted H_2O_2 solutions.

The structural parameters of dynamics related to the turbulence effects are carried out from the experimental data sets. The effective dynamical viscosity η is determined inside the channel at the real experimental condition for the different samples starting from the Washburn power law (Fig. S2a, equation 1) and writing the value of the pressure Δp according to the Laplace equation,

$$\Delta p = \frac{\gamma_{LV} \Delta \cos \theta}{R_H}$$

. The values for the structural and energy parameters such as hydraulic radius R_H , contact angle θ and the surface tension γ_{LV} have been directly measured (Table S2).

The Reynolds number (Re) is calculated as $Re = \rho v L / \eta$, with ρ the fluid density, v the fluid speed, L the device geometry and η the dynamical viscosity determined inside the channel at the real experimental condition for the different samples (see Fig. S2b). Finally, we determined the Weissenberg number, $Wi = v \lambda / L$, where λ is related to the relaxation time of the system. Weissenberg number is a dimensionless number which describes the degree of nonlinearity in the mechanical properties (Fig. S2c).

The trend of η , Re and Wi as function of the time during the flow inside the microchannel for all the solutions are reported in Fig. S2 for all samples at different concentration of H_2O_2 and are compared with the behaviour of pure water used as reference. Even for pure water (black dotted curve of Fig. S2a), the viscosity η shows a dependence on the time because of strong *localization phenomena*^{4,5}. The effect is amplified when Ru_4POM -PMCs and H_2O_2 are added because the liquid becomes viscoelastic and behaves as a non-Newtonian fluid. In the case of water (black dotted curve), very low values of Re and Wi , due to a purely laminar regime, are calculated; the addition of Ru_4POM -PMCs introduces a strong effect and determine an increase of the Re and Wi values with a parabolic profile during the flow time.

Figures

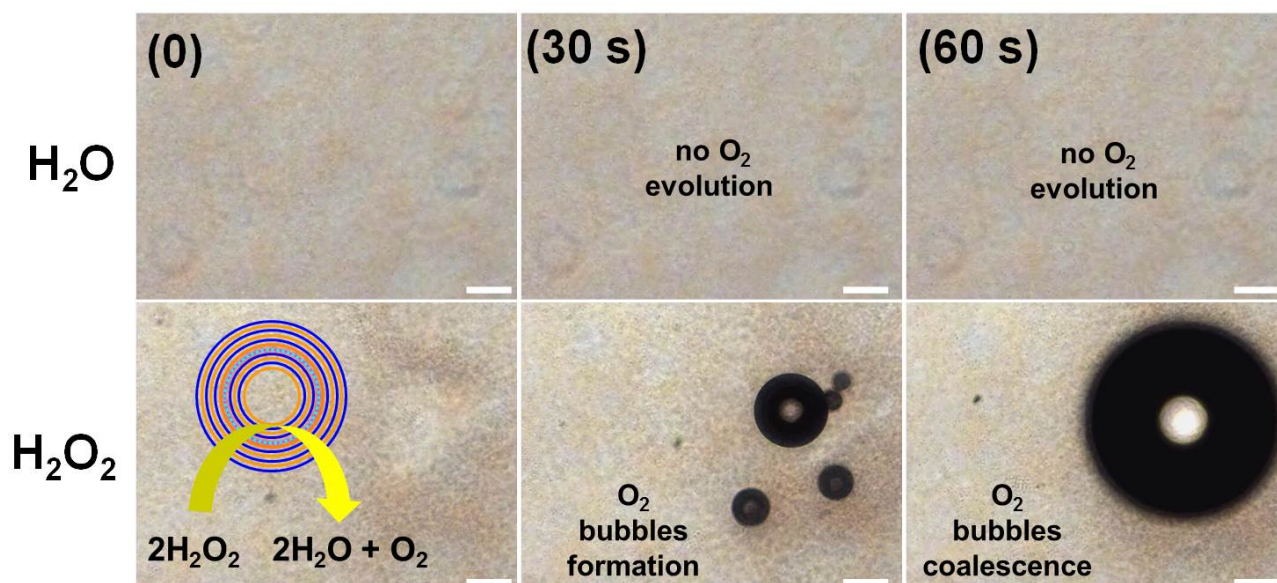


Figure S1. Time-lapse images of $(\text{PSS/PAH})_2\text{Ru}_4\text{POM}(\text{PSS/PAH})_3$ capsules in H_2O (Top) and in H_2O_2 (30% H_2O_2 , Bottom) at 0, 30, and 60 s, respectively. Scale bars 100 μm . In order to record the formation and evolution of the O_2 bubbles, a low magnification objective was used (10x). At such magnification the microcapsules with average diameter of 3-4 μm can't be detected as individual objects.

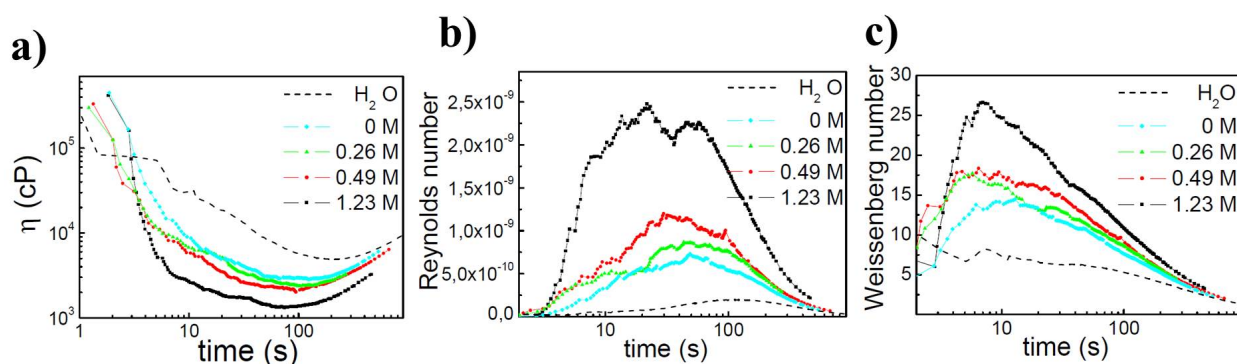


Figure S2. a) η , b) Re , and c) Wi trends as function of time for pure water (black dotted curve) and the $\text{Ru}_4\text{POM-PMCs}$ solutions of 0, 0.26, 0.49 and 1.23 M H_2O_2 .

1. A. A. Darhuber, S. M. Troian and W. W. Reisner, *Physical Review E*, 2001, **64**, 031603.
2. I. Viola, D. Pisignano, R. Cingolani and G. Gigli, *Analytical Chemistry*, 2004, **77**, 591-595.
3. M. Bianco, I. Viola, M. Cezza, F. Pietracaprina, G. Gigli, R. Rinaldi and V. Arima, *Microfluid Nanofluid*, 2012, **13**, 399-409.
4. D. Sinton, L. Ren and D. Li, *Journal of Colloid and Interface Science*, 2003, **260**, 431-439.
5. M. D. Graham, *Physics of Fluids (1994-present)*, 2003, **15**, 1702-1710.

Video S1. The video shows the meniscus movement in the microchannel for a 0.49 M H_2O_2 solution. As soon as the droplet is deposited at the inlet, it starts flowing through the channel. Some PMCs, probably aggregates, are visible, being the scale too large to visualize single PMCs. Each segment in the ruler corresponds to 50 μm . During the flow, the meniscus shows acceleration and deceleration which suggests a "spring effect".